Compact quantum cascade laser based quartz-enhanced photoacoustic spectroscopy sensor system for detection of carbon disulfide

Johannes P. Waclawek, Harald Moser, and Bernhard Lendl*

Institute of Chemical Technologies and Analytics, Vienna University of Technology, Getreidemarkt 9/164-UPA, 1060 Vienna, Austria

**bernhard.lendl@tuwien.ac.at*

Abstract: A compact gas sensor system based on quartz-enhanced photoacoustic spectroscopy (QEPAS) employing a continuous wave (CW) distributed feedback quantum cascade laser (DFB-QCL) operating at 4.59 μm was developed for detection of carbon disulfide (CS_2) in air at trace concentration. The influence of water vapor on monitored QEPAS signal was investigated to enable compensation of this dependence by independent moisture sensing. A 1 σ limit of detection of 28 parts per billion by volume (ppbv) for a 1 s lock-in amplifier time constant was obtained for the CS_2 line centered at 2178.69 cm^{-1} when the gas sample was moisturized with 2.3 vol% H_2O. The work reports the suitability of the system for monitoring CS_2 with high selectivity and sensitivity, as well as low sample gas volume requirements and fast sensor response for applications such as workplace air and process monitoring at industry.

OCIS codes: (140.5965) Semiconductor lasers, quantum cascade; (300.6340) Spectroscopy, infrared; (280.4788) Optical sensing and sensors; (110.5125) Photoacoustics.

References and links

1. *Ullmann's Encyclopedia of Industrial Chemistry* (Wiley-VCH, 2011), Chap. Carbon Disulfide.
2. Agency for Toxic Substances and Disease Registry, *Toxicological Profile for Carbon Disulfide*, (U.S. Department of Health and Human Services, Public Health Service, 1996).
3. R. Newhook and M. E. Meek, *Carbon Disulfide* (WHO, 2002).
4. *NIOSH Pocket Guide to Chemical Hazards* (NIOSH Publication, 2007).
5. S. S. Sehnert, L. Jiang, J. F. Burdick, and T. H. Risby, "Breath biomarkers for detection of human liver diseases: Preliminary study," Biomarkers **7**(2), 174–187 (2002).
6. M. A. Kamboures, D. R. Blake, D. M. Cooper, R. L. Newcomb, M. Barker, J. K. Larson, S. Meinardi, E. Nussbaum, and F. S. Rowland, "Breath sulfides and pulmonary function in cystic fibrosis," Proc. Natl. Acad. Sci. U.S.A. **102**(44), 15762–15767 (2005).
7. M. Phillips, "Detection of carbon disulfide in breath and air: a possible new risk factor for coronary artery disease," Int. Arch. Occup. Environ. Health **64**(2), 119–123 (1992).
8. R. F. Curl, F. Capasso, C. Gmachl, A. A. Kosterev, B. McManus, R. Lewicki, M. Pusharsky, G. Wysocki, and F. K. Tittel, "Quantum cascade lasers in chemical physics," Chem. Phys. Lett. **487**(1–3), 1–18 (2010).
9. A. Miklós, P. Hess, and Z. Bozóki, "Application of acoustic resonators in photoacoustic trace gas analysis and metrology," Rev. Sci. Instrum. **72**(4), 1937–1955 (2001).
10. A. A. Kosterev, Y. A. Bakhirkin, R. F. Curl, and F. K. Tittel, "Quartz-enhanced photoacoustic spectroscopy," Opt. Lett. **27**(21), 1902–1904 (2002).
11. J. P. Waclawek, R. Lewicki, H. Moser, M. Brandstetter, F. K. Tittel, and B. Lendl, "Quartz-enhanced photoacoustic spectroscopy-based sensor system for sulfur dioxide detection using a CW DFB-QCL," Appl. Phys. B **117**(1), 113–120 (2014).
12. Y. Ma, G. Yu, J. Zhang, X. Yu, R. Sun, and F. Tittel, "Quartz enhanced photoacoustic spectroscopy based trace gas sensors using different quartz tuning forks," Sensors (Basel Switzerland) **15**(4), 7596–7604 (2015).
13. S. Viviani, M. Siciliani de Cumis, S. Borri, P. Patimisco, A. Sampaolo, G. Scamarcio, P. De Natale, F. D'Amato, and V. Spagnolo, "A quartz-enhanced photoacoustic sensor for H_2S trace-gas detection at 2.6 μm," Appl. Phys. B **119**(1), 21–27 (2014).
14. A. A. Kosterev, F. K. Tittel, D. Serebryakov, A. L. Malinovsky, and I. Morozov, "Applications of quartz tuning forks in spectroscopic gas sensing," Rev. Sci. Instrum. **76**(4), 043105 (2005).

#257542 Received 19 Jan 2016; revised 17 Feb 2016; accepted 17 Feb 2016; published 15 Mar 2016

15. L. Dong, A. A. Kosterev, D. Thomazy, and F. K. Tittel, "QEPAS spectrophones: design, optimization, and performance," Appl. Phys. B **100**(3), 627–635 (2010).
16. G. Wysocki, A. A. Kosterev, and F. K. Tittel, "Influence of molecular relaxation dynamics on quartz-enhanced photoacoustic detection of CO_2 at λ =2 μm," Appl. Phys. B **85**(2–3), 301–306 (2006).
17. T. L. Cottrell and J. C. McCoubrey, *Molecular Energy Transfer in Gases* (London Butterworths, 1961).
18. Y. Yao, A. J. Hoffman, and C. F. Gmachl, "Mid-infrared quantum cascade lasers," Nat. Photonics **6**(7), 432–439 (2012).
19. Pacific Northwest National Laboratory, "Gas-phase databases for quantitative infrared spectroscopy," (2004), http://nwir.pnl.gov/
20. S. Schilt and L. Thévenaz, "Wavelength modulation photoacoustic spectroscopy: theoretical description and experimental results," Infrared Phys. **48**(2), 154–162 (2006).
21. P. Patimisco, A. Sampaolo, L. Dong, M. Giglio, G. Scamarcio, F. K. Tittel, and V. Spagnolo, "Analysis of electro-elastic properties of custom quartz tuning forks for optoacoustic gas sensing," Sens. Actuators B Chem. **227**, 539–546 (2016).

1. Introduction

Carbon disulfide (CS_2) is being used as a raw material in a variety of industrial applications, at which the production of regenerated cellulose in form of rayon fibers and cellophane is the dominant industrial use, accounting for three-fourth of the total demand [1]. Other important application areas of CS_2 are the synthesis of tetrachloride and the production of sulfur compounds including agricultural and rubber chemicals. Detection of this molecule down to sub-parts per million by volume (ppmv) concentration levels is of big interest for process monitoring and control, as well as for health protection at workplace in industrial environments, as this is the main route of human exposure [2]. CS_2 is extensively absorbed by inhalation and also by skin with critically health hazards since it acts as a neurotoxin [3]. The United States regulatory permissible exposure limit (PEL) value of CS_2 directed by the Occupational Safety and Health Administration (OSHA) is 20 ppm expressed as a time-weighted average for an 8-hour workshift of a 40-hour workweek. The advisory PEL value recommended by the National Institute of Occupational Safety and Health (NIOSH) is even 1 ppm, and the immediately dangerous to life or health (IDHL) concentration in ambient air is 500 ppm [4].

Other application areas where sensitive CS_2 detection could be used is medical diagnostics, in terms of breath analysis and environmental monitoring. Increased levels of CS_2 in exhaled breath have been found to indicate cirrhosis and it is a potential noninvasive marker of respiratory bacterial colonization in cysitic fibrosis [5, 6]. Regions with elevated CS_2 concentration levels can trigger the development of atherosclerosis and coronary artery disease by prolonged exposure [7]. Laser based spectroscopy is a powerful tool, capable of detection of a various number of molecules with high selectivity and sensitivity. To the best of the authors knowledge neither sensitive laser based spectroscopy measurements with an analytical focus on quantifying CS_2 has been covered in the literature, nor an application of a laser based CS_2 sensor for industrial monitoring purposes is reported to date.

Quartz-enhanced photoacoustic spectroscopy (QEPAS) is a very powerful technique that allows selective and sensitive measurements of trace gases in an ultra-small acoustic detection module (ADM) with a total sample volume of only a few mm^3 [8]. The principle of this technique is based on the photoacoustic (PA) effect, where the absorption of modulated laser radiation by gas molecules causes a periodic heating of the chemical species. The heating results in thermal expansion, and leads to a pressure change in the targeted media. The generated pressure wave can be detected by an acoustic transducer, which may be a broadband condenser or electrets microphone in case of conventional PA spectroscopy, or a quartz tuning fork (QTF) in case of QEPAS [9, 10]. The QTF is a sharply resonant piezoelectric element designed for the use as timing oscillator in electronic clocks. In vacuum the resonance frequency of the QTF is 32,768 (= 2^{15}) Hz and the quality factor can exceed 10^5. It can be used as acoustic transducer since it converts its deformation, caused by generated pressure waves, into separation of electrical charges that can be measured as a voltage. The small size of the QTF (~5.5 × 1.5 × 0.3 mm) enables cell geometries with

#257542 Received 19 Jan 2016; revised 17 Feb 2016; accepted 17 Feb 2016; published 15 Mar 2016

extremely low volume, which is very advantageous on the one hand if just little sample gas volume is present and on the other hand if fast sensor response with minimized signal diversion during online monitoring is desired. Only the fundamental symmetric vibration of the QTF is piezoelectric active, i.e. when the two prongs bend in opposite directions in the plane of the QTF. Therefore, in a typical QEPAS arrangement the laser beam is focused between the two prongs of the QTF in order to probe the acoustic waves and achieve the highest electric signal [10–16]. This property also results in excellent environmental noise immunity, as sound waves from distant acoustic sources tend to move the QTF prongs in the same direction, thus resulting in no electrical response. Moreover, QEPAS possesses a large dynamic range, a wide temperature and pressure range, and its noise is limited by thermal noise of the QTF [14]. A significant enhancement of the detected QEPAS signal can be achieved when two tubes acting as a micro-resonator (mR) are added to the QTF sensor architecture [15]. The generation of a photoacoustic wave is related to the vibrational-translational (V-T) relaxation in gases, i.e., the energy transfer from vibrationally excited molecular states to translational degrees of freedom [16]. Water vapor is known to be an effective catalyst for the vibrational energy transfer reaction in the gas phase, thus enhancing the QEPAS response of slow relaxing molecules, which results in higher amplitude of the detected signal [17]. The dependence of the amplitude of the acoustic wave on the water concentration is a disadvantage of the QPEAS technique. However, there are possibilities easy to implement in order to compensate this dependence, such as simultaneous measurement of the sample gas humidity.

Quantum cascade lasers (QCLs) are semiconductor devices based on intersubband transitions of electrons in multiple-quantum-well structures [18]. The QEPAS technique benefits from the use of QCLs because they can be designed to emit light at a particular wavelength in the region from ~3 to 25 μm, where strong fundamental ro-vibrational transitions in molecules can be excited. The QCL technology also assures small sized devices, which come with high optical power. The combination of a QCL with QEPAS enables an overall small sensor system size suitable for portable devices.

Due to the unique advantages of the QEPAS technique it is suited for a variety of applications with the need for selective trace gas detection. In this work the metrological qualities of CS_2 detection by the QEPAS technique are investigated. Moreover, a compact and robust sensor system is presented, capable for continuous monitoring of this molecule in an industrial environment.

2. Experimental

2.1 Quantum cascade laser (QCL) performance

In this work a high heat load (HHL) packaged continuous wave (CW) distributed feedback quantum cascade laser (DFB-QCL) (*HHL-14-15, AdTech Optics*) emitting radiation at a center wavelength of 4.59 μm was utilized as a compact light source. The DFB-QCL was continuously single mode tunable, generating up to 75 mW of optical radiation. The HHL package comprised an aspheric lens in order to collimate the beam. Frequency tuning over a few wavenumbers could be accomplished by varying the QCL temperature either by the thermoelectric cooler (TEC) or the injection current. Coarse frequency tuning over 2.36 wavenumbers (2179.21 - 2176.85 cm^{-1}) at a fixed maximum injection current of 280 mA and voltage of 12.2 V could be achieved by varying the laser temperature by 15 K (288.15 – 303.15 K), which corresponds to the measured laser temperature tuning coefficient of −0.157 cm^{-1} K^{-1}. Fine frequency tuning at a fixed TEC temperature in the range of 1.3 cm^{-1} could be performed by changing the injection current with an investigated current tuning coefficient of −0.013 cm^{-1} mA^{-1}. The optical power was measured by a commercial power meter (*Solo 2, Gentec-Eo*). Figure 1(a) depicts the emitted single mode laser radiation spectra at different QCL currents but constant temperature of 292.6 K obtained by a Fourier transform infrared

#257542 Received 19 Jan 2016; revised 17 Feb 2016; accepted 17 Feb 2016; published 15 Mar 2016

(FT-IR) spectrometer (*Vertex 80v, Bruker Corp.*) with an instrumental spectral resolution of 0.075 cm^{-1}. The inset presents the injection current and voltage characteristics as well as the optical power characteristics of the CW-DFB-QCL at the same fixed temperature together with highest achievable optical power at 288.15 K. Figure 1(b) shows the collimated QCL beam profile at a distance of 50 cm recorded with a pyroelectric array camera (*Pyrocam III, Spiricon, Ophir Photonics*).

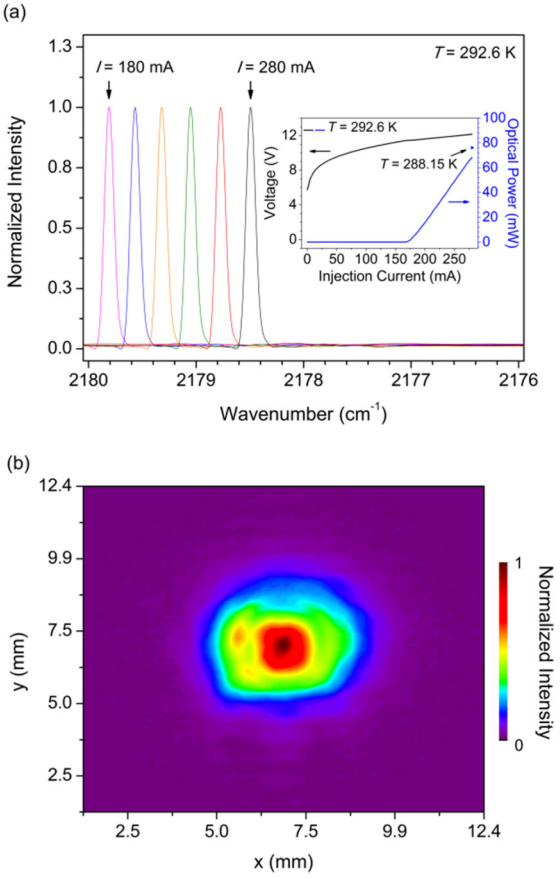

Fig. 1. (a) Single mode QCL output radiation for six injection currents at a fixed temperature of 292.6 K; Inset: CW-DFB-QCL output power, injection current and voltage characteristics at fixed QCL temperature together with highest achievable power at different QCL temperature; (b) 2D beam profile at a distance of 50 cm (I = 250 mA, T = 292.6 K).

In order to minimize the influence of the ambient temperature on the emitted QCL frequency, the HHL package was enclosed by an aluminum casing whose temperature was controlled by another TEC. The hot side of the TEC was attached to a heat sink, which in turn was cooled by a fan. In addition, this temperature stabilized enclosure also enabled an easy investigation on the dependence of the HHL package temperature on the emitted frequency. This could be realized by measuring the emitted frequency while changing the enclosure temperature at a fixed QCL temperature. Figure 2 shows the obtained FT-IR spectra when the HHL package temperature was varied within the range of 16 K at a fixed QCL temperature and current. For comparison the current tuning characteristics at fixed QCL and housing temperature are shown as well. The results demonstrate an observed package temperature tuning coefficient of 0.028 $cm^{-1}K^{-1}$, which is clearly far too large if the envisioned portable

#257542 Received 19 Jan 2016; revised 17 Feb 2016; accepted 17 Feb 2016; published 15 Mar 2016

sensor system operates at different ambient temperatures. Especially thinking of PAS, where the detectable signal is directly proportional to the irradiated optical power, high QCL power is essential for achieving best sensitivity. Therefore, it is crucial to probe the sample with best achievable parameters. The active temperature control of the HHL package minimizes the influence of ambient temperature changes considerably. However, it is obvious that the HHL package cannot be isolated perfectly from the environment because of heat transfer between air and housing on the not isolatable sides, where the optical window and connectors are located. The inset in Fig. 2 shows an illustration of the enclosed HHL packaged QCL mounted on a heat sink.

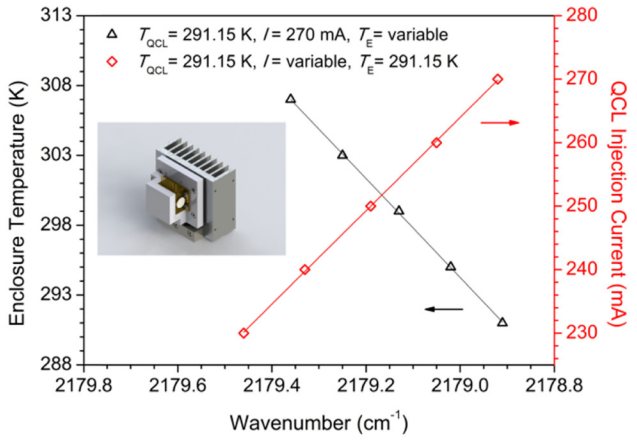

Fig. 2. Dependence of the HHL package temperature on the emitted QCL frequency at fixed QCL temperature and injection current; Inset: Illustration of the HHL packaged QCL and the enclosure for temperature stabilization by a TEC mounted on a heat sink.

2.2 Carbon disulfide (CS_2) wavelength selection

Selection of an adequate CS_2 absorption line for selective spectroscopic measurements was carried out by measured FT-IR spectra, as no HITRAN data set for this molecule exists and therefore simulation of a spectrum is not possible. Figure 3(a) shows a measured absorption spectrum of CS_2 in the spectral region from 6500 to 600 cm^{-1} [19]. The strongest absorption of CS_2 occurs between 1550 cm^{-1} and 1500 cm^{-1}, with the strongest line centered around 1542 cm^{-1}. Unfortunately, no CW-DFB-QCL covering a line in this region was commercially available at the time when this project was started. Hence, the region with second strongest absorption lines in the range from 2200 to 2140 cm^{-1} was chosen, as here QCLs which were originally designed for CO analysis were commercial available. In order to perform sensitive CS_2 QEPAS measurements the absorption line centered at 2178.69 cm^{-1} (Fig. 3(a), inset) was chosen. This line shows a ~44 times weaker absorbance compared to the strongest CS_2 line. An absorption spectrum at reduced pressure (p = 75 mbar) was measured using a FT-IR spectrometer together with a white cell having an optical path length of 21.75 m. Figure 3(b) depicts the measured absorption spectrum of 10 ppmv CS_2 in N_2 together with HITRAN2008 simulated spectra of 2.5 vol% H_2O and 10 ppmv CO also at an absolute pressure of 75 mbar within the spectral range covered by the CW-DFB-QCL. In order to perform selective CS_2 QEPAS measurements the absorption line centered at 2178.69 cm^{-1} and a QCL temperature of 296.2 K was selected, because of its relative strong line intensity and absent CO and H_2O interferences as well as high achievable laser power.

#257542 Received 19 Jan 2016; revised 17 Feb 2016; accepted 17 Feb 2016; published 15 Mar 2016

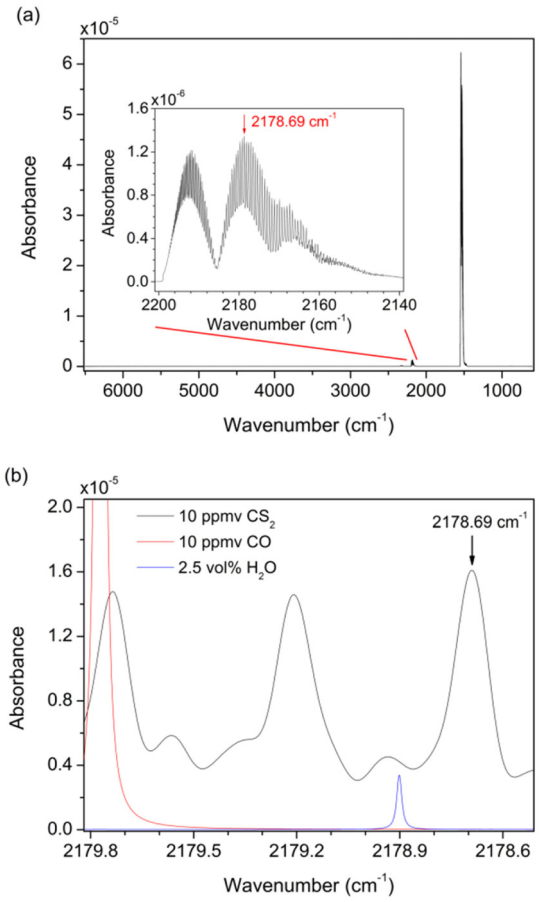

Fig. 3. (a) Measured spectrum of 1 ppm-cm CS_2 (p = 1013.25 mbar) [19]; (b) Measured spectra of CS_2 together with HITRAN2008 simulated spectra of CO and H_2O within the wavelength tuning range of the QCL at an absolute pressure of 75 mbar.

2. 3 Sensor system architecture and operation principle

A schematic of the QEPAS based gas sensor architecture employing a HHL packaged CW-DFB-QCL with collimation lens as coherent light source is depicted in Fig. 4. The beam was focused with a plano-convex CaF_2 lens (f = 40 mm) into a compact QEPAS ADM gas cell, which consisted of two anti-reflective coated ZnSe windows, the QTF used as an acoustic transducer and connectors for gas in- and outlet. Signal enhancement due to acoustic coupling between the components was achieved by adding two tubes to the QTF sensor architecture acting as a micro-resonator (mR). Two 4.4 mm long stainless steel tubes with 0.9 mm inner diameter were positioned closely before and after the QTF forming a typical QEPAS spectrophone configuration. The inner diameter of the acoustic resonator tubes differ about 300 µm from experimental determined optimum parameters [15], because when using mid-IR free space optics a larger inner diameter of the tubes is acceptable to simplify the alignment of the excitation beam through the mR tubes without large reduction of the QEPAS signal. In order to set up the simplest optical arrangement, the QCL beam was adjusted through the QTF and micro-resonator tubes by one plano-convex CaF_2 lens (f = 40 mm). Highest transmission efficiency of more than 99.5% was achieved when the lens was placed at a distance of 50 cm from the QCL source. The total volume of the ADM was 5.7 cm^3 and could easily be further reduced to a few mm^3, since the volume of the analyzed gas is only limited by the dimensions

#257542 Received 19 Jan 2016; revised 17 Feb 2016; accepted 17 Feb 2016; published 15 Mar 2016

of the QTF and the acoustic mR. The Q-factor of the QTF used in this work was ~27046 with a corresponding frequency f_0 = 32,760.79 Hz at a total pressure of 75 mbar.

After the ADM the QCL beam was again collimated by another CaF_2 plano-convex lens (f = 40 mm) and guided through a reference cell (*Wavelength References Inc.*) filled with 30% CS_2 in N_2 at a pressure of 75 mbar onto a photoconductive two stage thermoelectrically cooled MCT-detector (*PCI-2TE-12 / MPAC-F-100*, *Vigo Systems S.A.*). The gas cell and the detector were used as reference channel which makes it possible to lock the laser frequency to the center of the selected CS_2 absorption line using the 3f signal. The sensor platform was based on 2f wavelength modulation spectroscopy (WMS) and QEPAS detection [20]. The 2f WMS operation mode provides suppression of the acoustic background caused by nonselective absorbers, whereby the noise level of the sensor is primarily determined by the thermal noise of the QTF. However, additional noise can be introduced by unintended illumination of the QTF by laser light, including any scattered light and incidental reflections from optical elements.

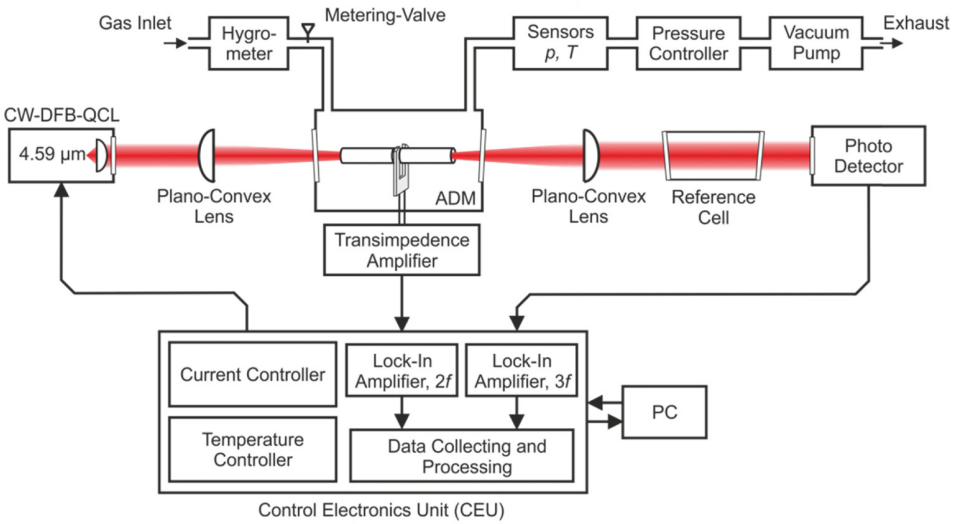

Fig. 4. Schematic diagram of the QEPAS based sensor employing a CW-DFB-QCL.

In order to implement the 2f WMS technique the emission wavelength of the CW-DFB-QCL was modulated at half of the QTF resonance frequency $f_{mod} = f_0 / 2$ by adding a sinusoidal modulation to the direct current (DC) input of the laser. The detection of the QTF signal was performed at f_0, using an internal lock-in amplifier (LIA) with the time constant set to 1 second. The QEPAS detection was performed in two modes: scan mode and locked mode. In the scan mode, the DC component of the QCL current is slowly tuned (mHz) so the laser frequency sweeps over the desired spectral range in order to acquire spectral information of the gas sample. In the locked mode, the QCL frequency is locked to the center of the CS_2 absorption line at 2178.69 cm^{-1} to avoid any laser drift and to ensure stable long-term measurements by demodulating the 3f component of the PD signal with a LIA. The DC component of the QCL is adjusted proportionally to maintain the laser frequency at the center of the absorption line. A piezoelectric current is generated in the QTF when acoustic waves interact with the element causing vibration of its prongs. The piezoelectric current was converted to a voltage by an ultra-low noise transimpedance amplifier with a 10 MΩ feedback resistor and was subsequently transferred to a control and data processing electronics unit (*QEPAS Control Electronics Unit, CDP Systems Corp.*) which provides all basic functions for

#257542 Received 19 Jan 2016; revised 17 Feb 2016; accepted 17 Feb 2016; published 15 Mar 2016

carrying out QEPAS measurements [14]. Further data processing was carried out with a LabView based program by transferring the digitized data to a computer.

The pressure and flow of the sample gas inside the ADM was controlled and maintained by using a metering valve, a mini diaphragm vacuum pump and a pressure controller. The flow of the sample gas was kept at a constant rate of 25 ml min^{-1}. Pressure, humidity and temperature were measured by sensors in the gas line located before and after the ADM.

All components needed for performing QEPAS measurements, data acquisition and processing including power supplies for all devices were assembled into a compact housing with the dimension of 48 × 33 × 23 cm. Communication to the system and monitoring of the measured data could be carried out via a touch display, which was connected to the internal mainboard. Figure 5(a) shows a photograph of the compact QEPAS system with the gas in- and outlet and the touch display at the front side as well as the computer interfaces at the right side during measurement. Figure 5(b) shows a photograph of the optical platform which was placed inside the system. The beam was folded by two protected plane gold mirrors and sent afterwards through the ADM and the reference cell prior deflection onto the photodiode by another mirror.

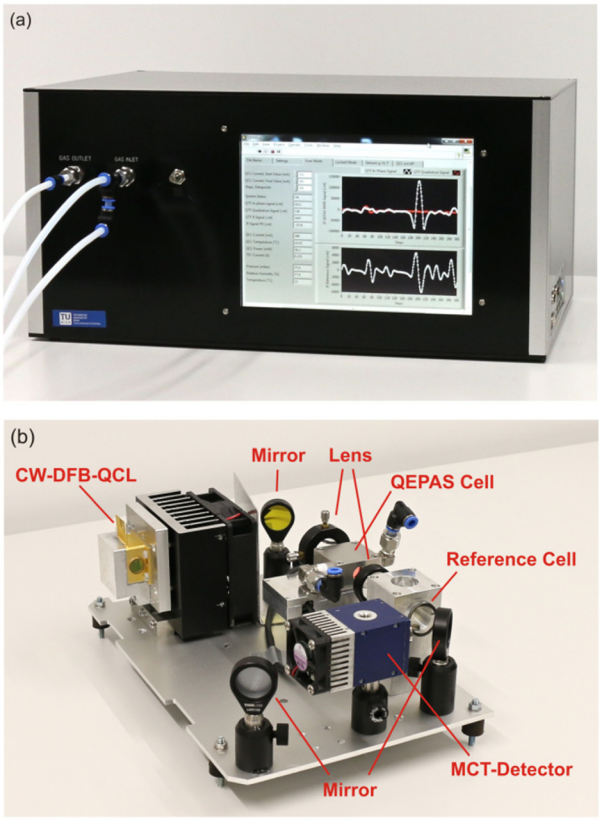

Fig. 5. (a) Compact QEPAS sensor system; (b) Optical platform of the setup.

3. Experimental results and discussion

3.1 Determination of optimum QEPAS operating parameters

The sensitivity of the QEPAS sensor is a function of the gas pressure p and the QCL wavelength modulation depth m. In order to identify the optimum operating conditions in terms of the highest 2f WMS signal amplitudes, a two-parameter sensor optimization (p and

#257542 Received 19 Jan 2016; revised 17 Feb 2016; accepted 17 Feb 2016; published 15 Mar 2016

m) was performed for a dry and a moisturized gas mixture. Certain CS_2 concentration levels were achieved by diluting a 50 ppmv CS_2:N_2 calibration mixture with ultra-high purity N_2 using a custom-made gas mixing system. The N_2 used for dilution could be moisturized with water vapor up to ~90% of relative humidity when passing N_2 through the gas phase of temperature controlled H_2O bath. CS_2 QEPAS signal amplitudes were recorded for different pressure levels within the range from 50 to 700 mbar. At each pressure level the QTF parameters f_0 and Q were measured and the QEPAS laser modulation depth was varied in the range between 0.5 mA and 8.5 mA, which corresponded to 0.007 cm^{-1} and 0.111 cm^{-1}. Figure 6(a) shows a comparison of the optimization curves for a dry and a humidified sample, at this pressure where the highest signal amplitude was found. Additionally, the characteristic for a dry sample at 75 mbar is shown to illustrate the dependence of the CS_2 QEPAS signal on sample gas humidity. The optimum working pressure and modulation depth for dry sample gas of CS_2:N_2 was found to be 300 mbar and 0.111 cm^{-1}, respectively, whereas optimum *p* and *m* for CS_2 in moisturized N_2 with 2.3 vol% H_2O was found to be 75 mbar and 0.026 cm^{-1}.

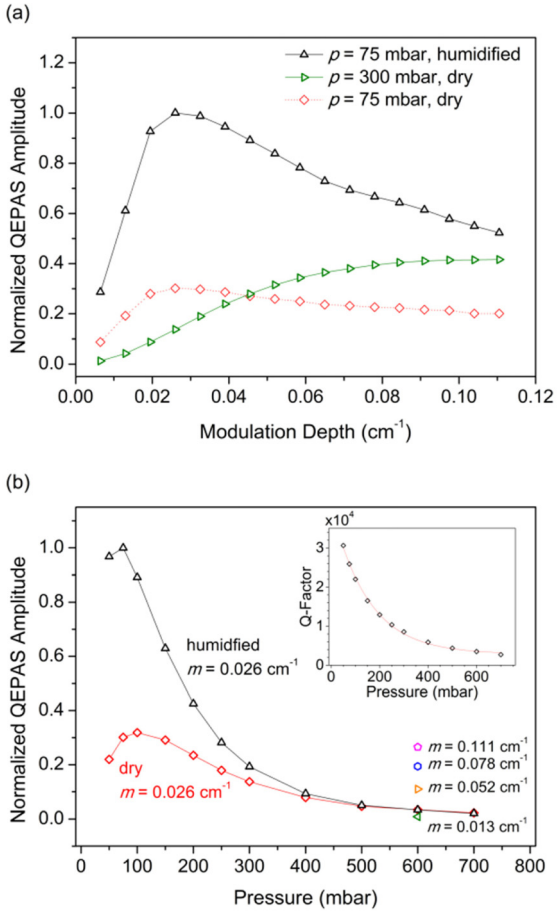

Fig. 6. (a) Sensor optimization curve for 10 ppmv CS_2 in dry and moisturized (c_{H2O} = 2.3%) N_2 in each case at the pressure where the highest QEPAS signal amplitude was found. For comparison the signal amplitudes of a dry sample are shown additionally at optimum pressure for a humidified sample to emphasize the dependence on water vapor. (b) Dependence of the CS_2 QEPAS signal amplitude on the sample gas pressure at a fixed modulation depth *m*. The signal amplitude at different modulation depths at a pressure of 600 mbar is shown as well. At this pressure level and above no influence of H_2O on the signal amplitudes were observed; Inset: Dependence of the Q-factor on the sample gas pressure.

#257542 Received 19 Jan 2016; revised 17 Feb 2016; accepted 17 Feb 2016; published 15 Mar 2016

The difference between the optimum working conditions for the two situations is due to the V–T relaxation mechanisms, which are different in the two mixtures because of the different pressures and water content. In the dry gas mixtures at low pressure the V-T relaxation is slow with respect to the modulation frequency. Therefore, the generated photoacoustic wave is weaker than it would be in case of instantaneous V-T energy equilibrium. Optimum working conditions can be found at higher pressure levels, since an increase of the relaxation rate is achieved by an increase of the gas pressure. On the other hand the QTF Q-factor decreases with increasing pressure, which causes the detected QEPAS signal to decrease.

For a humid CS_2 gas mixture the optimum working pressure shifted to lower pressure levels in respect to a dry gas mixture. The presence of H_2O vapor influenced the QEPAS response to CS_2 by enhancing the V-T energy transfer rate. As previously, the QTF Q-factor increases at reduced pressures and the impact of these effects result in the sensor optimization curve shown in Fig. 6. The Q-factor decreases from a value of more than 30600 at 50 mbar to 2700 at 700 mbar (see inset Fig. 6(b)). The shift of the resonance frequency is 5.76 Hz for this pressure range.

Figure 6(b) shows the QEPAS signal amplitudes for a dry and humidified gas mixture of 10 ppmv CS_2:N_2 at constant modulation depth m but different pressure levels. Above and at a pressure of 600 mbar no dependence on water vapor was observed. Highest signal amplitude where no dependence on the V-T relaxation is present can be found at 600 mbar and a modulation depth of 0.111 cm^{-1}.

In practical applications the analyte often needs to be quantified in a gas mixture with unknown water content. To correct for the dependence on water different approaches can be adapted: the sample gas can be humidified before analysis, or, the water content can be measured independently either with a hygrometer or with QEPAS itself. If the sample is humidified to nearby 100% relative humidity before analysis, the sensor system sensitivity will be highest at optimum working conditions due to the enhancement of the V-T relaxation rate. This approach can be realized by using a membrane for humidifying the sample gas. However, this approach entails disadvantages like increased need of sample gas volume, different permeability coefficients of various gases - which is in case of CS_2 2.5 times higher than for water for a polydimethylsiloxane membrane - and additional maintenance requirements. In contrast, a more convenient approach in terms of robustness and compactness of the total system is to monitor the sample gas humidity by a sensor. This can be achieved by using a hygrometer or measuring the water content directly by QEPAS using a neighboring water absorption line. However, this method is more time consuming because two different absorption lines have to be probed alternately and hence is not applicable if high temporal resolution is needed. An approach without taking care of the water content is to choose operation conditions where the V-T relaxation does not have any influence on the signal amplitude (compare Fig. 6(b)). This solution, however, is afflicted with a decrease in sensitivity. A further possibility would be to use a QTF with lower resonant frequency [21], where the photoacoustic sound generation is more efficient for sample gas systems with low V-T relaxation rates.

3.2 Influence of water vapor on the CS_2 QEPAS signal at sensor operation conditions

As discussed above, the presence of water vapor increases the relaxation rate of slow relaxing molecules such as CS_2 and therefore improves the QEPAS response to this molecule by increasing the signal amplitude. As also discussed above, there are different possibilities to compensate for varying water contents. Because the setup is designed for applications where it is expected that the sample gas will have high water contents, the system is characterized in the following only for optimum operation conditions for humidified sample gas, i.e. p = 75 mbar and m = 0.026 cm^{-1}, respectively, simply because of highest achievable

#257542 Received 19 Jan 2016; revised 17 Feb 2016; accepted 17 Feb 2016; published 15 Mar 2016

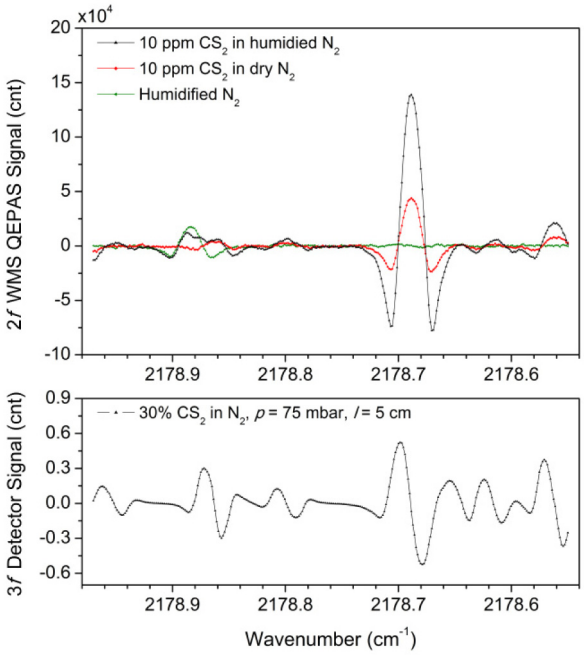

Fig. 7. Top: 2*f* WM QEPAS signals for 10 ppmv CS_2 in dry and moisturized N_2, as well as moisturized N_2 without CS_2 (c_{H2O} = 2.3%), when the QCL was tuned across the absorption line located at 2178.69 cm^{-1} (p = 75 mbar, m = 0.026 cm^{-1}); Below: 3*f* WM spectrum of the reference cell, detected by a photodetector.

sensitivity. The water content will be measured by a hygrometer. Therefore, the QEPAS response to different water contents must be investigated accurately. Calibration data based on the present study can be used to convert measured values into actual analyte concentrations. Figure 7 shows a comparison of 2*f* WMS QEPAS spectra of 10 ppmv CS_2 in dry and moisturized N_2 together with a spectrum of moisturized N_2 without CS_2 when the CW-DFB-QCL emission wavelength was tuned across the CS_2 absorption line centered at 2178.69 cm^{-1}. The spectral scan of the humidified N_2 confirms no spectral interference by water at the targeted absorption line.

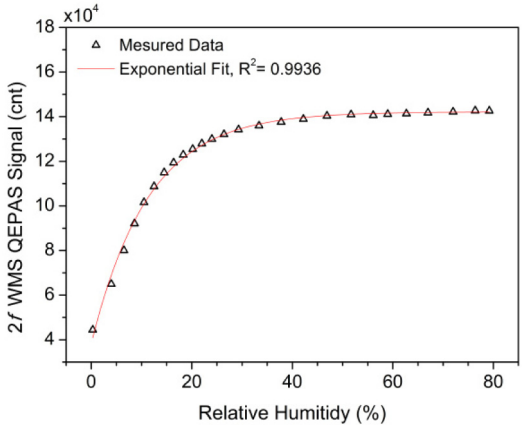

Fig. 8. 2*f* WM QEPAS signal amplitudes of 10 ppmv CS_2 as a function of H_2O concentration (p = 75 mbar, m = 0.026 cm^{-1}).

#257542 Received 19 Jan 2016; revised 17 Feb 2016; accepted 17 Feb 2016; published 15 Mar 2016

The dependence of the H_2O concentration on the response of the QEPAS based CS_2 sensor system was investigated in more detail by acquiring 2*f* WMS signals of the 10 ppmv CS_2 sample gas as a function of the H_2O concentration. The results shown in Fig. 8 indicate an improvement of the QEPAS signal by a factor 3.21 when the analyzed gas mixture was humidified with 2.3 vol% H_2O, which corresponds to 80.8% relative humidity, as opposed to a dry sample. The measured dependence is used to compensate different water contents by simultaneous measurement of the humidity with an additional sensor.

3.3 Sensitivity and linear response of the QEPAS based CS_2 sensor system

For the selected CS_2 absorption line centered at 2178.69 cm^{-1} the measured optical power emitted by the CW-DFB-QCL was ~62.6 mW (T = 292.6 K, I = 270 mA). The laser beam was focused between the mR and the gap of QTF prongs with a transmission efficiency of > 99.6%. Taking the absorption of the plano-convex lens (2.3%) and the optical window (5.3%) of the ADM into account an optical power of 57.7 mW was directed through the QTF prongs. The evaluation of the QEPAS sensor sensitivity and linearity as a function of the CS_2 concentration for humidified gas mixtures was investigated by continuous monitoring of stepwise concentration measurements within the range of 0 to 10 ppmv in the mode where the QCL was locked to the center of the CS_2 absorption line. Each concentration step was measured for total time duration of 10 minutes acquiring 2*f* WMS signals with a frequency of 1 Hz. In order to allow the gas mixture concentration to stabilize, the QEPAS signal acquisition was stopped for 1 min when the CS_2 concentration was changed. The measurement results are illustrated in Fig. 9(a). Data for each step were averaged and yielded an excellent linearity between measured signal amplitudes and CS_2 concentrations with a calculated R-square value of 0.9998 (Fig. 9(b)).

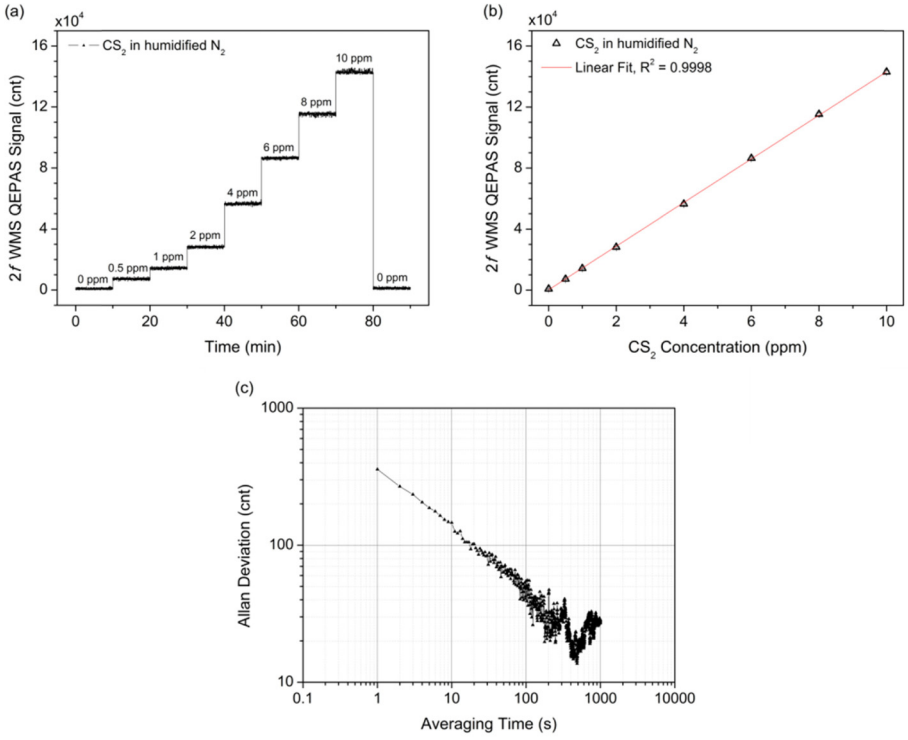

Fig. 9. (a) Stepwise concentration measurement of CS_2 in humidified N_2 with 2.3vol%; (b) Linear response of the QEPAS sensor; (c) Allan deviation plot for time series measurements of pure N_2.

#257542 Received 19 Jan 2016; revised 17 Feb 2016; accepted 17 Feb 2016; published 15 Mar 2016

Based on the calibration curve and the standard deviation of the noise level of pure N_2 a limit of detection (1 σ) of 28 ppbv for a 1 sec acquisition time was calculated. The corresponding normalized noise equivalent absorption (NNEA) coefficient was recalculated to be 8.12×10^{-9} cm^{-1} W $Hz^{-1/2}$.

To investigate the long-term stability of the CS_2 QEPAS sensor an Allan variance analysis was performed when pure N_2 was passed through the sensor while the QCL was locked to the CS_2 absorption line available via the reference gas cell. The Allan deviation plot depicted in Fig. 9(c) shows good stability of the sensor with an optimum averaging time of approximately 500 sec.

4. Conclusions

The results reported in this paper show that the CW-DFB-QCL based QEPAS sensor system offered sensitive and selective detection of CS_2 sufficient for practical applications at industry. For the CS_2 line centered at 2178.69 cm^{-1} a 1 σ limit of detection of 28 ppbv (τ = 1 s) was achieved when the sample gas was moisturized with 2.3 vol% water vapor. Improvement of the detection sensitivity could be realized by targeting the strongest CS_2 absorption line centered around 1542 cm^{-1}. Considering this option the minimum detection limit could be lowered by a factor of ~44 times. Furthermore, no adverse absorption of other gas molecules, such as H_2O or CO is present at the targeted absorption line and at the selected operation conditions. However, the acoustical cross-sensitivity of the sensor system to water due to its influence on the V-T relaxation of CS_2 has to be considered. Nevertheless, a strategy to solve this problem has been elaborated and successfully implemented.

In addition, a compact and portable sensor system has been assembled. The transition from a typical research set-up placed on an optical table into a compact sensor system is important for the planned use of this sensor system for process or workplace monitoring at industry as well as for environmental surveillance applications. In this regard special attention was also given to an accurate temperature control of the QCL housing even at strongly varying ambient temperatures to enable long-term stability of the sensor. Another compelling feature of the now available QEPAS CS_2 sensor system is its fast response time due to the small sample volume of the acoustic detection module, which along with the achieved detection sensitivity allows to measure quick changes in the CS_2 concentration of process gas streams. This feature will eventually allow tracing of so far unknown process details when sampling process gas streams of the Rayon industry.

Acknowledgments

JPW, HM and BL acknowledge financial support provided by the Austrian research funding association FFG under the scope of the COMET program within the research networks “Process Analytical Chemistry” (contract # 825340) and imPACts (contract # 843546) as well as the Carinthian Tech Research.

#257542 Received 19 Jan 2016; revised 17 Feb 2016; accepted 17 Feb 2016; published 15 Mar 2016